Am J Transl Res 2016;8(11):4657-4669
www.ajtr.org /ISSN:1943-8141/AJTR0036614

Original Article

Astragaloside IV enhances cardioprotection of remote ischemic conditioning after acute myocardial infarction in rats

Songyi Cheng[1], Peng Yu[2], Li Yang[1], Haibo Shi[2], Anxia He[3], Hanyu Chen[1], Jie Han[1], Liang Xie[4], Jiandong Chen[2], Xiaohu Chen[2]

[1]First Clinical Medical College, Nanjing University of Chinese Medicine, Nanjing 210023, P. R. China; Departments of [2]Cardiology, [3]Ultrasonography, Jiangsu Province Hospital of Traditional Chinese Medicine, The Affiliated Hospital of Nanjing University of Chinese Medicine, Nanjing 210029, P. R. China; [4]Department of Cardiology, Jinling Hospital, The Affiliated Hospital of Nanjing University, Nanjing 210002, P. R. China

Received July 25, 2016; Accepted November 12, 2016; Epub November 15, 2016; Published November 30, 2016

Abstract: Background: Remote ischemic conditioning (RIC) has been shown to be a practical method for protecting the heart from ischemic/reperfusion (I/R) injury. In the present study, we investigated whether or not the combination of RIC and Astragaloside IV (AS-IV) could improve cardioprotection against acute myocardial infarction (AMI)-induced heart failure (HF) when compared with individual treatments. Material and Methods: A rat model of AMI was established via permanent ligation of the left anterior descending coronary artery (LAD). Postoperatively, the rats were randomly grouped into a sham group (n=10), a model group (n=15), an AS-IV alone group (n=15), an RIC alone group (n=15) and a combined treatment group (AS-IV+RIC; n=15). All treatments were administered for 2 weeks. Results: After treatment for 2 weeks, the survival rate was improved, the cardiac function was preserved and the infarcted size was limited in AS-IV alone and RIC alone treatment groups compared to the model group, whereas the combined treatment yielded the most optimal protective effects. Additional studies suggested that AS-IV enhanced the cardioprotective effects of RIC by alleviating myocardial fibrosis, suppressing inflammation, attenuating apoptosis and ameliorating impairment of the myocardial ultrastructural. Conclusion: AS-IV enhances the cardioprotective effects of RIC against AMI-induced HF and ventricular remodeling, which represents a potential therapeutic approach for preserving cardiac function and improving the prognosis of AMI.

Keywords: Astragaloside IV, remote ischemic conditioning, acute myocardial infarction, ventricular remodeling, cardioprotection

Introduction

Acute myocardial infarction (AMI) remains a leading cause of morbidity and mortality in most developed countries worldwide. It has been estimated that approximately every 42 seconds, an American will experience an AMI [1]. Even though death rates have fallen due to medical treatments and changes in risk factors [2], patients who survive the acute AMI stage have an increased risk of post-AMI left ventricular remodeling and heart failure (HF). Current pharmacological strategies, such as inhibitors of the renin-angiotensin-aldosterone system (RAAS) and β-adreno receptor blockers, reportedly improve outcomes to some extent [3, 4], however, contraindications and adverse effects have limited their clinical application. Therefore, the development of a novel therapy which is both convenient to perform and well accepted is of great importance.

Ischemic preconditioning (IPC) is regarded as the most powerful endogenous protective strategy against AMI, which limits size of infarction and improves cardiac function [5]. Experimental studies over the past few decades have led to the identification of complex mechanisms underlying the cardioprotection afforded by IPC [6-8]. Nevertheless, the clinical application of IPC is restricted due to the requirement that the stimulus be provided prior to the onset of lethal ischemia, which is nearly impossible to predict [9]. Furthermore, the invasive intervention must

be applied directly to the coronary artery, which is only accessible during cardiac surgery or percutaneous coronary intervention (PCI). In addition, IPC might cause serious complications including coronary artery dissection, rupture of atheromatous plaques and distal embolism. Following researches have broadened the adaptability of ischemic conditioning therapy to allow transient ischemia/reperfusion (I/R) to be applied at the onset of reperfusion (ischemic postconditioning, IPOST) [10, 11], or at the distal tissue (remote ischemic conditioning, RIC) [12, 13]. However, studies have demonstrated that neither IPOST nor RIC yield adequate cardioprotective effects when compared to IPC [14-16].

Astragaloside IV (AS-IV), the major active component extracted from Huangqi (Radix Astragali Mongolici), exerts diverse pharmacological effects including suppression of inflammation, inhibition of oxidative stress, a reduction in apoptosis, as well as anti-viral effects [17-19]. Recently, the therapeutic effects of AS-IV on cardiovascular diseases were fully investigated, including potential protection against I/R injury, vascular endothelium dysfunction and bradycardia [20-22]. Our previous studies also revealed that AS-IV promoted angiogenesis and prevented lipopolysaccharide-induced injury [23, 24].

Several studies have demonstrated that the combination of ischemic conditioning therapy and pharmacological treatment during ischemia might result in more robust protection against I/R injury [25-27], however, whether combination therapy could enhance cardioprotection during AMI-induced HF has not been investigated despite the potential clinical significance. Thus, the aim of this study was to determine whether AS-IV combined with RIC produces stronger cardioprotective effects than each treatment administered separately using a rat model of AMI established by the permanent ligation of the left anterior descending coronary artery (LAD).

Material and methods

Rat model of AMI

A total of 90 adult male Sprague-Dawley rats weighing 250±20 g obtained from the Yangzhou University Comparative Medicine Centre (Yangzhou, China, Permission No.: 201512739) were used in this study. The animals were housed in clean cages in accordance with the guidelines of the Nanjing University of Chinese Medicine Animal Care and Use Committee and the animal protocol was approved following a review of the Lab Animal Use Application by the Nanjing University of Chinese Medicine Ethics Review.

Briefly, the induction of anesthesia was performed by an intraperitoneal injection of pentobarbital sodium (50 mg/kg) prior to surgery. The animals were then intubated and connected to a ventilator to maintain normal respiration. The surgical area was prepped and cleaned, and a left thoracotomy was performed. A 6-0 silk suture was placed between the pulmonary and left auricle where the LAD is located. The successful induction of AMI was confirmed based on the observation of the pale color of the anterior portion of the left ventricle and the appearance of AMI on the electrocardiogram oscilloscope. In the sham group, a silk suture was passed through the myocardium without occluding the LAD. After the procedure, the thoracic cavity was closed using 4-0 silk suture and the excess air was evacuated using a syringe.

Treatment protocol

The AS-IV was obtained from Nanjing Zelang Medical Technology Co., Ltd. (Nanjing, China; purity: greater than 98%). Postoperatively, the rats were randomly assigned to one of five groups including the sham group (n=10), the model group (n=15), the AS-IV alone group (n=15), the RIC alone group (n=15), and the combined treatment group (AS-IV+RIC; n=15). The AS-IV was administered intragastrically for 2 weeks (50 mg/kg/day). The rats in the RIC alone group received repeated transient limb ischemia with tourniquet: three cycles of left limb ischemia for 5 min followed by reperfusion for 5 min, the protocol was performed once a day for 2 weeks. The combined treatment group received both AS-IV and RIC for 2 weeks, whereas equal doses of normal saline were administered intragastrically once daily in the model, sham, and RIC groups.

Measurement of echocardiography

After treatment for 2 weeks, the heart structure and function were evaluated using a Siemens Acuson™ SC2000 high-frequency ultrasound

system (Siemens, Inc., Berlin, Germany). After the rats were anesthetized with pentobarbital, two-dimensional echocardiographic measurements were obtained. The left ventricular internal diastolic diameter (LVIDd), the left ventricular internal systolic diameter (LVIDs), the left ventricular ejection fraction (LVEF), and the left ventricular fractional shortening (LVFS) were measured and calculated from the M-mode tracing.

Evaluation of myocardial infarction size

Following euthanasia, hearts were collected from the rats and stored at -20°C for 20 min. The hearts were then cut into 2 mm slices across the long axis, incubated with 2% Triphenyltetrazolium chloride (TTC, Sigma, St Louis, USA) in phosphate-buffered saline (PBS) at 37°C for 30 min in the dark, and then fixed in 10% paraformaldehyde overnight. The infarcted site was pale white, whereas the normal tissue was brick-red. The tissue slices were imaged and the infarcted size was calculated using Image-Pro Plus 6.0 (Media Cybernetics, Silver. Spring, USA).

Test of histopathology and fibrosis

The rats' hearts were harvested and weighed after treatment for 2 weeks, washed in PBS, fixed in 4% paraformaldehyde overnight, and embedded in paraffin. Sections (4-μm-thick) were cut and stained with hematoxylin-eosin (H&E) and Masson's trichrome stain. Each section was imaged by microscopy (Nikon, Japan). The ratio of fibrotic area to the total area of connective and myocardial tissue was also calculated using Image-Pro Plus 6.0 (Media Cybernetics, Silver. Spring, USA).

Measurement of apoptosis by TUNEL/DAPI immunofluorescence

The number of apoptotic cells was quantified by terminal deoxynucleotidyl transferase (TdT)-mediated dUTP nick end labeling (TUNEL) staining using a fluorescence detection kit (Biouniquer, Nanjing China) in accordance with the manufacturer's instructions. Staining with 4',6-diamidino-2-phenylindole (DAPI; 1 mg/ml; Sigma, St Louis, USA) was used to assess nuclear morphology. The fluorescein isothiocyanate (FITC)-labeled TUNEL-positive cells were observed by fluorescence microscopy at 400× magnification. Image J software (NIH, Bethesda, MD, USA) was used to calculate the area of TUNEL and DAPI-positive staining.

Western blotting analysis

Apoptosis-associated proteins (Bax and Bcl-2) and inflammation-associated proteins (TLR4 and NF-κB) were measured by Western blotting. Total protein was extracted from the myocardial tissue and homogenized in RIPA buffer (Beyotime Institute of Biotechnology, Haimen, China). Quantitative analysis of protein concentration was conducted by bicinchoninic acid (BCA, Thermo Fisher Scientific, Waltham, USA) assay kit. 20 μg of total protein from each sample was electrophoresed and separated by 6-12% SDS-PAGE, then transferred onto polyvinylidene difluoride (PVDF, Millipore, Billerica, USA) membranes. The membranes were blocked with 5% Bovine serum albumin (BSA) for 60 min at room temperature, then incubated overnight at 4°C with primary antibodies including rabbit anti-Bax (1:1000; Abcam, Cambridge, MA, USA), rabbit anti-Bcl-2 (1:1000; Abcam, Cambridge, MA, USA), rabbit anti-NF-kB (1:800; Cell Signaling Technology, USA), rabbit anti-TLR4 (1:1000; Abcam, Cambridge, MA, USA), and rabbit anti-β-actin (1:800; Abcam, Cambridge, MA, USA). The PVDF membranes were then washed with TBST three times and incubated with HRP-conjugated secondary antibodies (1:2000; Abcam, Cambridge, MA, USA) in 5% BSA at room temperature for 60 min. The resulting bands were visualized using enhanced chemiluminescence (ECL) detection reagents (Thermo Fisher Scientific, Waltham, USA) according to the manufacturer's instructions, quantified using a chemiluminescence image analyzer (GE Healthcare Bio-Sciences, Pittsburgh, USA), and analyzed using Image J software (NIH, Bethesda, MD, USA). The protein expression was normalized using the expression of β-actin as a reference.

Assessment of ultrastructural impairment by transmission electron microscopy (TEM)

The hearts from the rats in each group were obtained following euthanasia, washed in PBS, cut into 1 mm^3 cubes, sequentially fixed in 4% glutaraldehyde and 4% osmium tetroxide for 24 h, dehydrated in acetone, embedded in paraffin resin, and then ultra-thin sections were acquired using a microtome and standard pro-

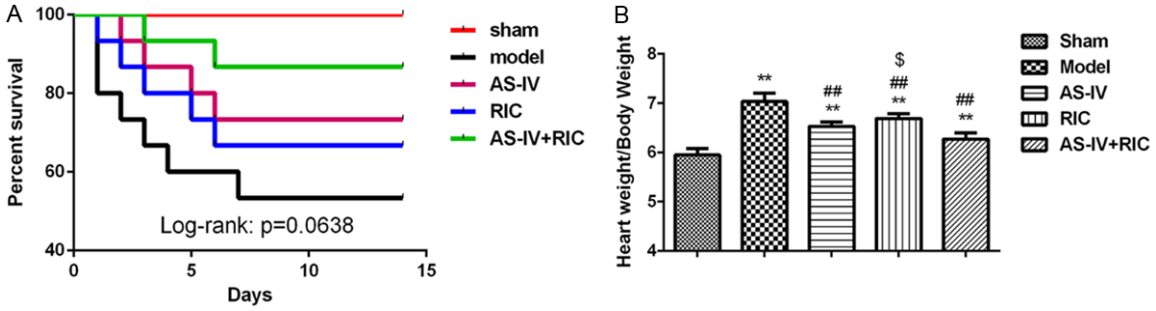

Figure 1. Survival rate and the heart/body weight ratio after treatment for 2 weeks. A: Kaplan-Meier analysis indicated the survival rates of the rats after AMI. The combination treatment group exhibited a trend towards improved overall survival rate 2 weeks after the induction of AMI, but differences did not reach statistical significance (log-rank: P=0.0638). B: Analysis of the heart weight/body weight ratio, data are expressed as the mean ± SD. **: P<0.01 versus sham group, ##: P<0.01 versus model group, $: P<0.05 versus combined treatment group.

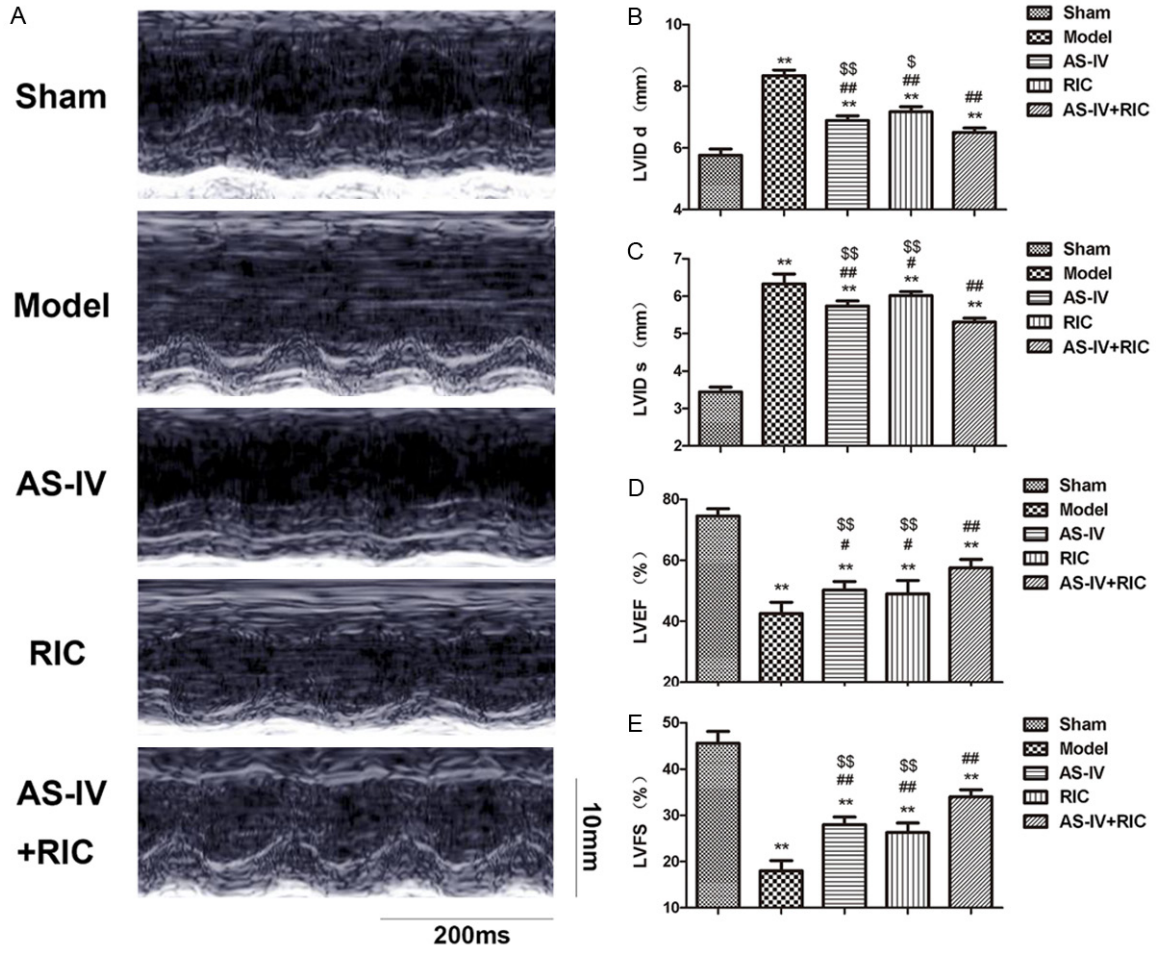

Figure 2. Cardiac function at the end of treatment. (A) M-mode echocardiographic images of the rats in all groups. The analysis of LVIDd (B), LVIDs (C), LVEF (D), and LVFS (E) 2 weeks after treatment was also conducted, which revealed that LVIDd and LVIDs were decreased, whereas LVEF and LVFS improved in the combined treatment group compared with the model group and the individual treatment groups. Data are expressed as the mean ± SD. **: P<0.01 versus sham group, #: P<0.05 versus model group, ##: P<0.01 versus model group, $: P<0.05 versus combined treatment group, $$: P<0.01 versus combined treatment group.

cedures (Leica, Germany). The sections were then stained with 1% uranyl acetate and 0.2% lead citrate. The sections were analyzed on a transmission electron microscope (TEM;

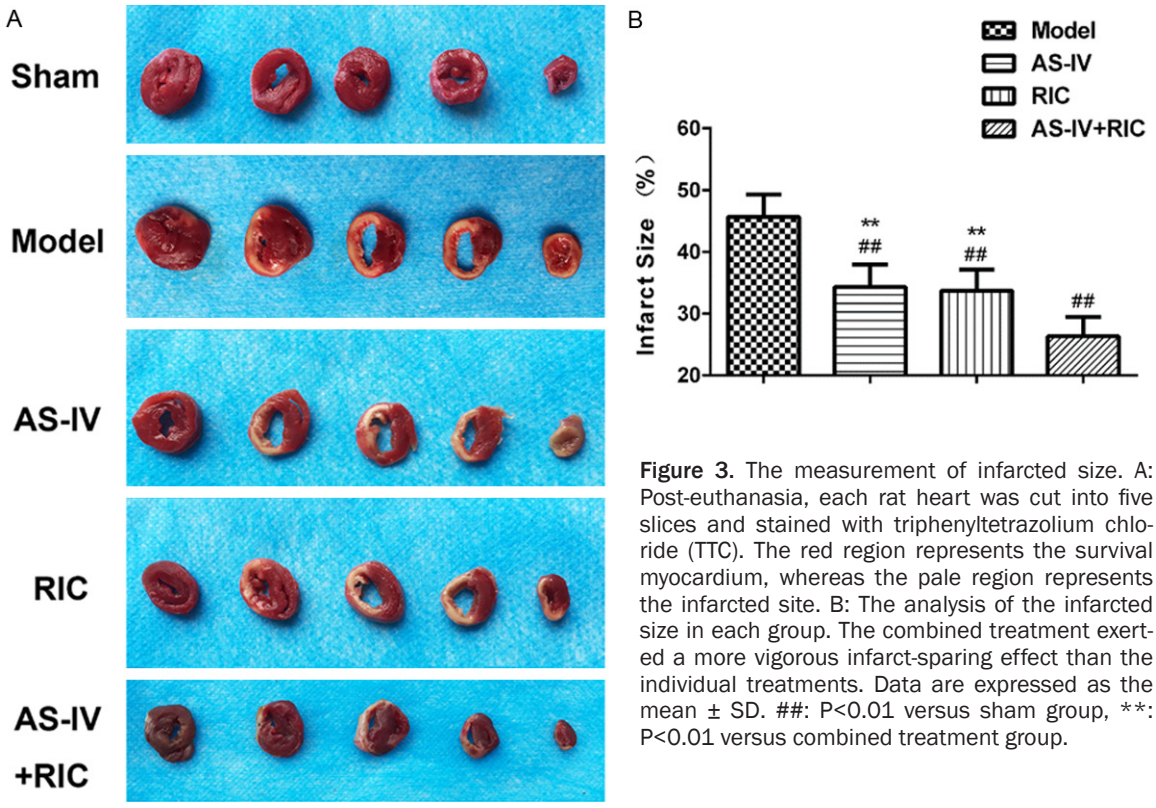

Figure 3. The measurement of infarcted size. A: Post-euthanasia, each rat heart was cut into five slices and stained with triphenyltetrazolium chloride (TTC). The red region represents the survival myocardium, whereas the pale region represents the infarcted site. B: The analysis of the infarcted size in each group. The combined treatment exerted a more vigorous infarct-sparing effect than the individual treatments. Data are expressed as the mean ± SD. ##: P<0.01 versus sham group, **: P<0.01 versus combined treatment group.

Hitachi, Japan) and images were acquired at 25000× magnification.

Statistical analysis

SPSS 22.0 and GraphPad Prism 5 software were used for statistical analysis and for generating graphs, respectively. All values are expressed as the mean ± standard error. One-way ANOVA and Tukey's test were utilized to evaluate the statistical differences between the groups and for post hoc analyses, respectively. A Kaplan-Meier survival analysis was used to evaluate the overall survival rates of the rats after treatment. A *P*-value <0.05 was considered statistically significant.

Results

RIC therapy alone or in combination with AS-IV treatment improved survival rate in rat after AMI

As shown in **Figure 1A**, rats in the sham group were not subjected to LAD ligation; thus, all of the rats survived after 14 days. However, nearly half of the rats in the model group died in the first week. Because pneumonedema was observed in most of the rats during the post-mortem examination, HF was deemed to be the main cause of death. Compared with the model group, the survival rates after AMI were 73.3% and 66.7% in the AS-IV and RIC groups, respectively. The survival rate in the combined treatment group was 86.7%, which indicated that the rats that received AS-IV and RIC had a better prognosis compared to the rats that were administered a single treatment. Nonetheless, although the trend indicated improved outcomes in the rats, it was not statistically significant across all treatment groups (Log-rank test P=0.0638).

RIC therapy alone or in combination with AS-IV treatment preserved heart function of rats after AMI

Two weeks after the induction of AMI, the results of two-dimensional echocardiography revealed impaired myocardial contractility, increased LVIDd/LVIDs, and lower LVFS/LVEF in the model group compared with the sham-operated group. Cardiac function was improved in the rats in all treatment groups; however, the combined treatment group exhibited a significant decrease (P<0.01, respectively) in LVIDd

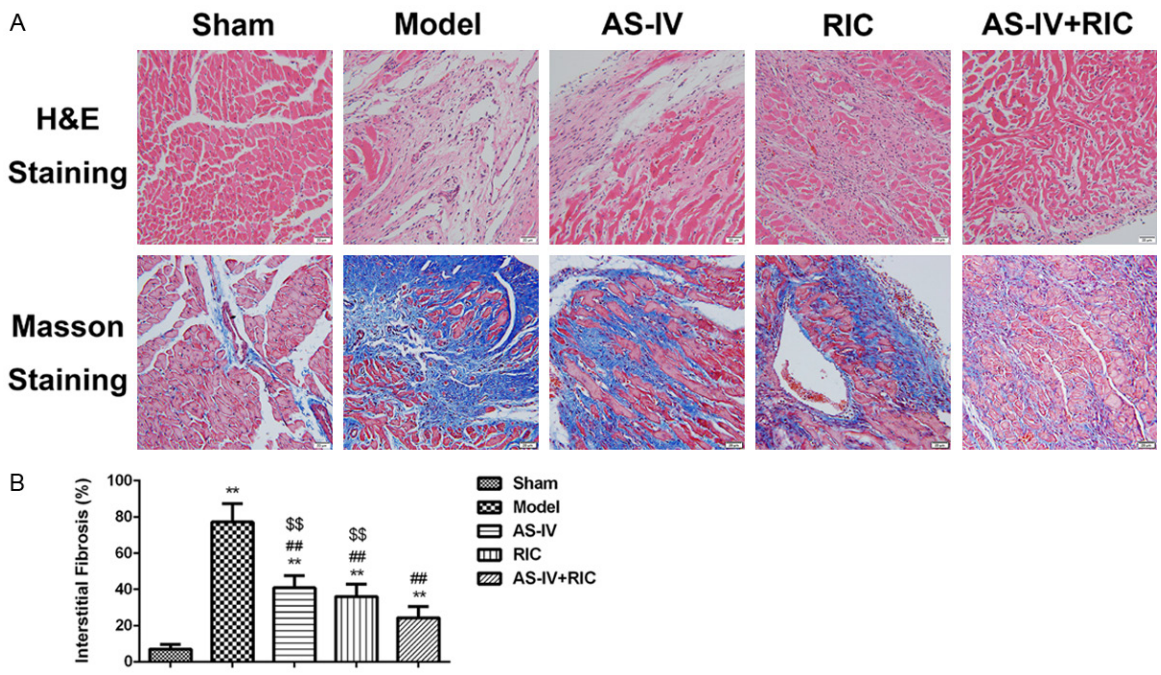

Figure 4. Evaluation of the pathological changes and interstitial fibrosis at 400× magnification. A: Representative images of H&E and Masson's trichrome staining of the hearts from rats with AMI. Necrotic tissue and poorly arranged cardiac myocytes were noted following H&E staining. In the Masson's trichrome stained sections, blue represents the collagen fiber. B: The quantitative analysis of areas of interstitial fibrosis after treatment. The rats in the combined treatment group exhibited the least pathological changes and a minimal ratio of fibrotic area to total area of connective and myocardial tissue compared with the individual treatment groups. Data are expressed as the mean ± SD. ##: P<0.01 versus sham group, **: P<0.01 versus combined treatment group, $$: P<0.01 versus combined treatment group.

and LVIDs and an increase in LVEF and LVFS compared with the other two treatment groups. No significant differences in LVIDd/LVIDs and LVFS/LVEF were observed between the RIC and AS-IV groups, although the rats in the AS-IV group appeared to have improved cardiac function (**Figure 2**). The heart weight/body weight (HW/BW) ratio was also evaluated after the rats were euthanized, which revealed that the ratio was significantly lower in the combined treatment group compared with the model, AS-IV, and RIC groups. Similarly, the difference between the RIC and AS-IV groups was not statistically significant (**Figure 1B**).

RIC therapy alone or in combination with AS-IV treatment reduced infarcted size

Hearts were collected from the rats after euthanasia, cut transversely into five slices, and stained with TTC. The survival cardiac muscle tissue stained brick-red, whereas the infarcted tissue could not be stained. As shown in **Figure 3**, RIC therapy alone significantly reduced the infarcted size compared to the model group (33.68±3.33% vs 45.68±3.43%). AS-IV therapy alone also reduced the infarcted size compared to the model group (34.32±3.43% vs 45.68±3.43%). There were no statistically significant differences in the infarcted size between the RIC and AS-IV groups. However, the infarcted size was markedly reduced in the combination therapy group compared with the model group (26.32±2.99% vs 45.68±3.43%), the RIC group (26.32±2.99% vs 33.68±3.33%), and the AS-IV group (26.32±2.99% vs 34.32±3.43%).

Pathological changes and fibrosis in myocardial tissue after treatment

H&E and Masson's trichrome staining were used to observe the pathological changes and fibrosis in the myocardial tissue. As shown in H&E staining (**Figure 4A**), necrotic tissue could be found in the model group, and surviving myocardial cells in the infarct border zones exhibited greater irregularity and disarray in comparison to the sham group. However, all of the treated groups exhibited improvements

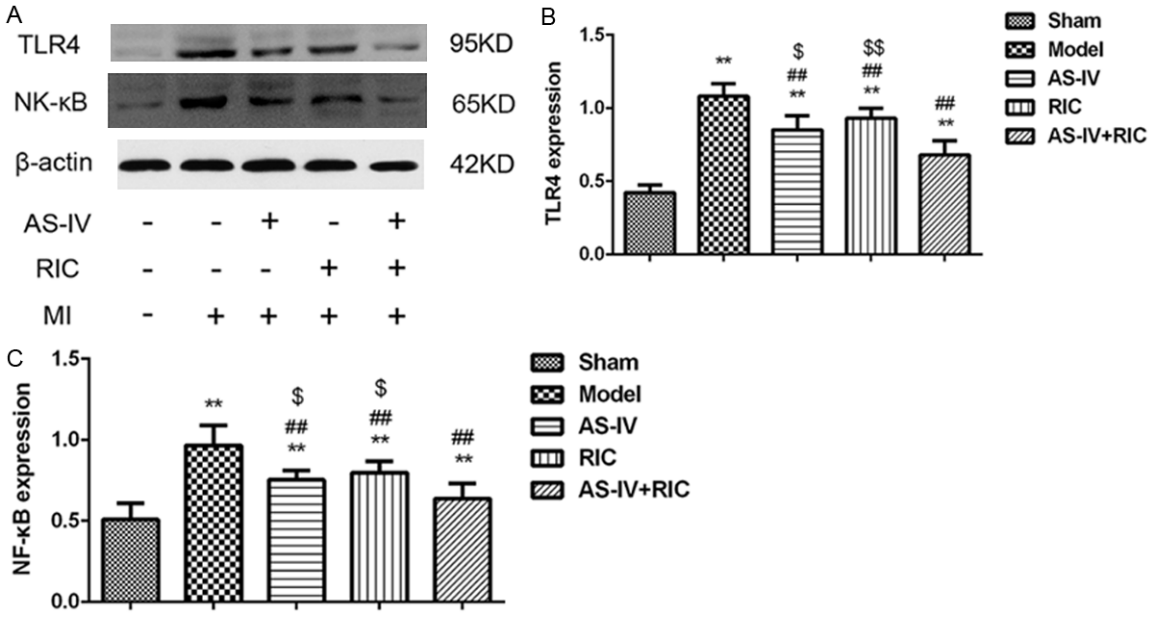

Figure 5. The expression of inflammatory factors after treatment. A: Western blotting analysis of the expression of TLR4 and its downstream protein NF-κB with β-actin as the internal control. B: Quantified western blot results of TLR4, which was normalized to the housekeeping gene β-actin. C: Quantified western blot results of NF-κB, which was normalized to the housekeeping gene β-actin. TLR4 and NF-κB were downregulated in all treatment groups to varying degrees, but the combined treatment yielded optimal anti-inflammatory effects. Data are expressed as the mean ± SD. **: P<0.01 versus the sham group, ##: P<0.01 versus the model group, $: P<0.05 versus the combined treatment group, and $$: P<0.01 versus the combined treatment group.

compared to the model group, including limited areas of necrosis, compact arrangement of the myocardial cells, and decreased inflammatory cells, with the combined treatment group displaying the highest degree of improvement. Further, the results of the Masson's trichrome staining demonstrated that both RIC and AS-IV efficiently decreased fibrosis and collagen deposition after AMI compared to the model group. Nonetheless, the combined treatment significantly alleviated (P<0.01) fibrosis and collagen deposition compared to the individual treatment groups (**Figure 4A** and **4B**).

RIC therapy alone or in combination with AS-IV treatment downregulated inflammatory cytokines after AMI

To determine if RIC therapy alone or in combination with AS-IV treatment suppressed the inflammatory response in rats with AMI, Western blotting was performed to determine the expression of TLR4 and its downstream protein NF-κB in myocardial tissues obtained from the rats. **Figure 5** shows that the model group had significantly higher levels of these two pro-inflammatory cytokines when compared to the sham-operated group; however, TLR4 and NF-κB were downregulated by both RIC therapy and AS-IV treatment alone as well as in combination. Nonetheless, no statistically significant differences in the protein levels were detected between the RIC and AS-IV treatment groups. However, the combination therapy significantly decreased the levels of TLR4 and NF-κB compared to the model group and to the individual treatments.

RIC therapy alone or in combination with AS-IV treatment decreases myocardium apoptosis after AMI

After treatment for 14 days, the expression of apoptosis-related factors was evaluated by Western blotting. The results indicated that the expression of Bax, a pro-apoptotic factor, was significantly downregulated, whereas the expression of Bcl-2, an anti-apoptotic factor, was significantly upregulated in both treatment groups (P<0.01, respectively), which contributed to an increased Bcl-2/Bax ratio compared with the model group (**Figure 6C-F**). Furthermore, we found that when RIC was combined with AS-IV treatment, a synergistic effect was

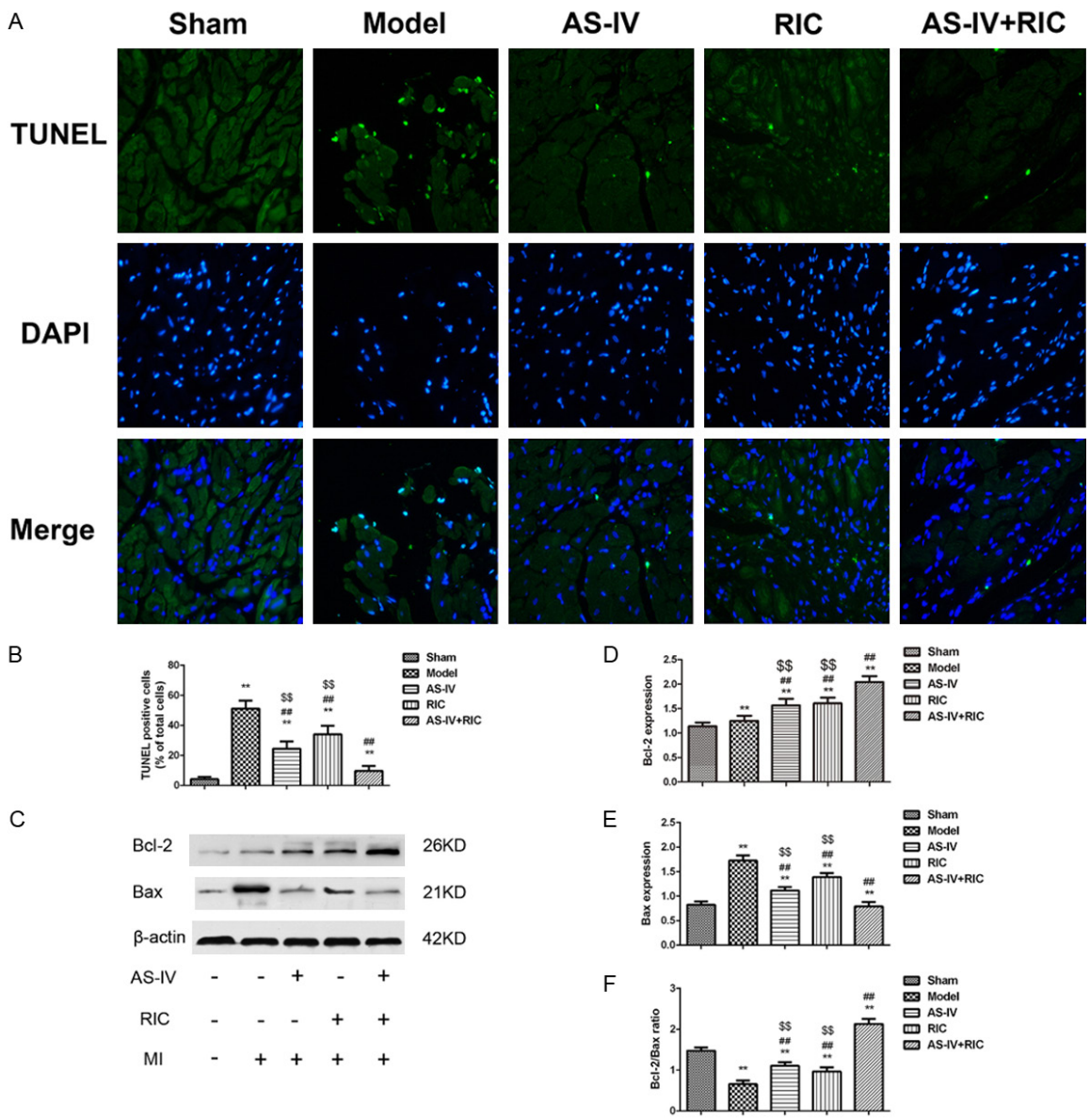

Figure 6. Assessment of myocardial apoptosis after treatment. (A) Representative graph of TUNEL/DAPI immunofluorescence at 400× magnification 2 weeks after AMI. The green fluorescence represents TUNEL-positive cells, whereas the blue fluorescence represents DAPI-positive cells. (B) The ratio of myocardial apoptosis (TUNEL-positive cells/DAPI-positive cells). Apoptosis was significantly inhibited by the combined treatment. (C) Expression of the apoptosis-related proteins Bcl-2 and Bax were measured by western blotting analysis, β-actin served as the internal control. Quantified western blot results of Bcl-2 (D), Bax (E), and the Bcl-2/Bax ratio (F) are provided. The combined treatment led to the downregulation of Bax and the upregulation of Bcl-2, which in turn led to an increased ratio of Bcl-2/Bax compared with the untreated and individual treatment groups. Data are expressed as the mean ± SD. **: P<0.01 versus the sham group, ##: P<0.01 versus the model group, and $$: P<0.01 versus the combined treatment group.

observed. Apoptosis in the border zone of the myocardium was also examined by TUNEL/DAPI immunofluorescence (**Figure 6A**). The apoptotic index of the model group was significantly higher than the corresponding index in the sham group (**Figure 6B**). When treated with RIC or AS-IV alone or with a combination of the two treatments, the number of TUNEL-positive cells observed in the infarcted myocardium declined to varying degrees compared with the model group; however, the combination therapy yielded the most robust protective effect, which was consistent with the altered trend in Bcl-2 and Bax expression.

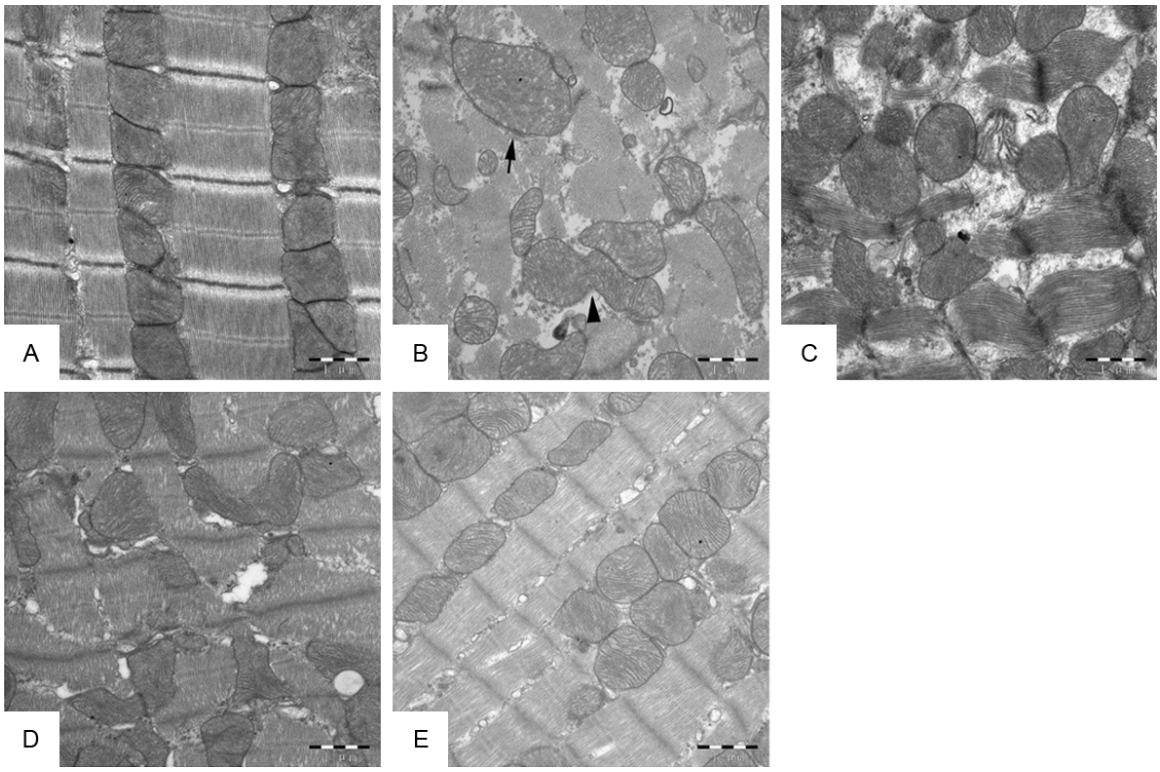

Figure 7. Observation of the ultrastructure performed by TEM at 25000× magnification. (A) The sham group. The myofilaments were neatly arranged and normal mitochondria were observed. (B) The model group. The structure of the myofilaments was barely visible, the mitochondria were markedly swollen, the mitochondrial cristae were fractured (arrows), and the fusion of the mitochondria (arrowheads) was likewise detected. The AS-IV (C) and RIC groups (D) exhibited fewer swollen mitochondria, and the structure of the myofilaments was somewhat improved. (E) The combined treatment group. The injury to the mitochondria and myofilaments was drastically reduced.

RIC therapy alone or in combination with AS-IV treatment ameliorated myocardium ultrastructural impairment after AMI

To obtain further insight into the contribution of RIC and AS-IV in regards to their apparent protective effects during AMI, ultrastructure morphometric assessments of the myocardium were conducted in each group by TEM at a magnification of 25000× (**Figure 7**). As indicated, the myofilaments were arranged in an orderly manner and the mitochondrial structure was undamaged in the sham-operated group. However, the structure of the myofilaments was disrupted, the mitochondria were markedly swollen, the mitochondrial cristae were fractured, and vacuolar degeneration and fusion of the mitochondria were noted in the model group. Additionally, the density of the mitochondria was decreased compared to the sham group, which collectively suggests that the ultrastructural impairment was severe in the model group. Treatment with RIC and AS-IV dramatically reduced the extent of the mitochondrial injury, decreased the ratio of mitochondrial swelling, and improved the organization of the myofilament alignment. Hence, the combination therapy yielded optimal effectiveness, in that irregular arrangement of the myofilaments was rarely observed and the mitochondrial injury was minimal, which correlated with the apparent macro pathological changes.

Discussion

Recent studies have indicated that RIC is a potentially effective strategy for alleviating left ventricular remodeling induced by AMI [28]. Compared to IPC, the application of RIC is thought to be more feasible in clinical practice because the protocol can be applied to a remote site using a blood pressure cuff, by increasing the pressure 20 mmHg greater than the patient's systolic blood pressure (SBP), and by leaving the cuff inflated for a specified amount of time prior to deflation [29]. Despite

the major advantages of RIC, its capacity for cardioprotection appears inferior to IPC and IPOST [14-16]. Hence, increasing the cardioprotection afforded by RIC should be clinically relevant.

In the present study, treatment with RIC and AS-IV alone or in combination improved the overall survival rate 2 weeks after the induction of AMI. Further, although the rats in the combined therapy treatment group demonstrated the most optimal outcomes, the differences between the treatment groups were not statistically significant. The results of echocardiography revealed that RIC therapy combined with AS-IV offered the most robust protection against the deterioration of systolic dysfunction and ventricular dilation. Consistently, the measurement of infarcted size by TTC staining suggested that the combination treatment exerted powerful infarct-sparing effects. All the data obtained support the hypothesis that AS-IV reinforces the cardioprotective effects of RIC in terms of attenuating cardiac remodeling and improving the outcome after AMI.

After the occurrence of AMI, necrotic cardiomyocyte death induced by hypoxia and ischemia invokes a series of events referred to as myocardium fibrosis, which can prevent further damage and rupture of the ventricular wall via preservation of the remaining cells and replacement of the dead cells [30, 31]. However, this compensative fibrosis takes place not only in the infarct border zone but also in the remote, undamaged myocardium, which leads to reduced chamber compliance and increased ventricular stiffness and thereby progressive development of HF [32]. Therefore, the ability to confine fibrosis to some degree represents an attractive target for therapeutic intervention. Prior reports in different systems with various mechanisms have indicated that AS-IV has anti-fibrotic properties [33-35], whereas only a limited number of studies have focused on the anti-fibrotic role of RIC. In the present study, our data indicate that the combined use of RIC and AS-IV treatment yielded a beneficial anti-fibrotic effect, which contributed to improved recoveries after AMI.

The TLR4/NF-κB signaling pathway is a crucial pro-inflammatory factor that is involved in the pathological progression of AMI, myocardial fibrosis, and ventricular remodeling [36-38]. Moreover, excessive inflammation or fibrosis has been linked to an increased incidence of arrhythmia and other AMI-related pathologies [39, 40]. In the present research, we observed the upregulation of inflammatory factors in rats with AMI and subsequent myocardial remodeling, which was in accord with previous research [41, 42]. We also demonstrated that each treatment downregulated the increased expression of TLR4/NF-κB; however, the lowest expression levels were observed with the combined treatment, which indicated that AS-IV might augment the cardioprotective properties of RIC with respect to the anti-inflammatory activity.

It should be noted that apoptosis has been shown to play a pivotal role in HF after AMI. In addition, the gradual reduction in cardiomyocytes is related to progressive thinning of the infarcted site, ventricular dilatation, and the occurrence of symptomatic HF [43]. Increasing evidence suggests that ischemic-induced apoptosis contributes to other forms of programmed cell death, including autophagic myocardial cell death [44, 45]. The results of our study suggest that the combined treatment yielded more robust inhibition of apoptosis after the onset of AMI in a rat model compared to the individual treatments. The latent mechanism might involve the upregulation of Bcl-2 and the inhibition of Bax, which was confirmed to play a critical role in the process of apoptosis [46]. Similarly, the ratio of myocardial apoptosis in the border regions, as demonstrated by TUNEL/DAPI immunofluorescence, correlated with the expression of apoptotic factors.

In addition, ultrastructural impairment, which reflects injury to the mitochondria and myofilaments, was also evaluated in the current study. A growing number of studies have reported persuasive evidence that mitochondrial dysfunction might be closely involved in the progression of hypertrophy and HF [47]. As shown in our research, AS-IV treatment enhanced the protective effects of RIC with respect to mitochondrial injury compared to the untreated group. In fact, myofilament injury, which is associated with the contractility of cardiac muscle fibers, was the mildest in the combined treatment group compared with the other treatment groups.

To the best of our knowledge, this is the first study to demonstrate the efficacy of RIC thera-

py alone and in combination with AS-IV in a chronic AMI model, which is clinically relevant. Our findings indicate that the combination of RIC and AS-IV could be a promising and effective strategy against the progression of heart remodeling and HF after AMI. However, our study had several limitations. First, the coordinated therapeutic effects might involve multiple signaling pathways and there could be overlap and crosstalk in these signaling pathways caused by the activation of both therapies; thus, further studies are required to determine the definitive relationship between the different pathways. Second, the intensity of the cardioprotective effects induced by RIC was associated with tissue volume and a protocol that entailed a specific ischemic stimulus, duration of ischemia, and times of the cycles [48]. Hence, whether different RIC protocols will yield different protective effects against post-AMI ventricular remodeling requires further investigation. Third, the evaluation of survival rate in this study did not yield statistically significant differences due to the limited sample size.

In conclusion, the results of the present study demonstrate that AS-IV enhanced the cardioprotective effects of RIC after AMI with respect to alleviating myocardial fibrosis, suppressing inflammation, reducing apoptosis, and ameliorating myocardial ultrastructural impairment, which led to a further reduction in myocardial injury and improved outcomes compared with the individual treatments. However, the mechanism behind the protective effects of the combined pharmacological treatment and RIC requires further investigation.

Acknowledgements

This work was supported by the grants from National Natural Science Foundation of China (NSFC) 81273943 and 81573908.

Disclosure of conflict of interest

None.

Address correspondence to: Drs. Xiaohu Chen and Jiandong Chen, Department of Cardiology, Jiangsu Province Hospital of Traditional Chinese Medicine, The Affiliated Hospital of Nanjing University of Chinese Medicine, Hanzhong Road 155#, Nanjing 210029, Jiangsu, P. R. China. E-mail: chenxhdoctor@sina.com (XHC); lamala@126.com (JDC)

References

[1] Mozaffarian D, Benjamin EJ, Go AS, Arnett DK, Blaha MJ, Cushman M, Das SR, de Ferranti S, Despres JP, Fullerton HJ, Howard VJ, Huffman MD, Isasi CR, Jimenez MC, Judd SE, Kissela BM, Lichtman JH, Lisabeth LD, Liu S, Mackey RH, Magid DJ, McGuire DK, Mohler ER 3rd, Moy CS, Muntner P, Mussolino ME, Nasir K, Neumar RW, Nichol G, Palaniappan L, Pandey DK, Reeves MJ, Rodriguez CJ, Rosamond W, Sorlie PD, Stein J, Towfighi A, Turan TN, Virani SS, Woo D, Yeh RW and Turner MB. Heart Disease and Stroke Statistics-2016 Update: A Report From the American Heart Association. Circulation 2016; 133: e38-60.

[2] Ford ES, Ajani UA, Croft JB, Critchley JA, Labarthe DR, Kottke TE, Giles WH and Capewell S. Explaining the decrease in U.S. deaths from coronary disease, 1980-2000. N Engl J Med 2007; 356: 2388-2398.

[3] Ram CV. Angiotensin receptor blockers: current status and future prospects. Am J Med 2008; 121: 656-663.

[4] Ibanez B, Macaya C, Sanchez-Brunete V, Pizarro G, Fernandez-Friera L, Mateos A, Fernandez-Ortiz A, Garcia-Ruiz JM, Garcia-Alvarez A, Iniguez A, Jimenez-Borreguero J, Lopez-Romero P, Fernandez-Jimenez R, Goicolea J, Ruiz-Mateos B, Bastante T, Arias M, Iglesias-Vazquez JA, Rodriguez MD, Escalera N, Acebal C, Cabrera JA, Valenciano J, Perez de Prado A, Fernandez-Campos MJ, Casado I, Garcia-Rubira JC, Garcia-Prieto J, Sanz-Rosa D, Cuellas C, Hernandez-Antolin R, Albarran A, Fernandez-Vazquez F, de la Torre-Hernandez JM, Pocock S, Sanz G and Fuster V. Effect of early metoprolol on infarct size in ST-segment-elevation myocardial infarction patients undergoing primary percutaneous coronary intervention: the Effect of Metoprolol in Cardioprotection During an Acute Myocardial Infarction (METOCARD-CNIC) trial. Circulation 2013; 128: 1495-1503.

[5] Otani H. Ischemic preconditioning: from molecular mechanisms to therapeutic opportunities. Antioxid Redox Signal 2008; 10: 207-247.

[6] Lundberg KC and Szweda LI. Preconditioning prevents loss in mitochondrial function and release of cytochrome c during prolonged cardiac ischemia/reperfusion. Arch Biochem Biophys 2006; 453: 130-134.

[7] Das DK, Engelman RM and Kimura Y. Molecular adaptation of cellular defences following preconditioning of the heart by repeated ischaemia. Cardiovasc Res 1993; 27: 578-584.

[8] Mayr M, Metzler B, Chung YL, McGregor E, Mayr U, Troy H, Hu Y, Leitges M, Pachinger O, Griffiths JR, Dunn MJ and Xu Q. Ischemic preconditioning exaggerates cardiac damage in

PKC-delta null mice. Am J Physiol Heart Circ Physiol 2004; 287: H946-956.
[9] Hausenloy DJ and Yellon DM. The therapeutic potential of ischemic conditioning: an update. Nat Rev Cardiol 2011; 8: 619-629.
[10] Zhao ZQ and Vinten-Johansen J. Postconditioning: reduction of reperfusion-induced injury. Cardiovasc Res 2006; 70: 200-211.
[11] Laskey WK. Brief repetitive balloon occlusions enhance reperfusion during percutaneous coronary intervention for acute myocardial infarction: a pilot study. Catheter Cardiovasc Interv 2005; 65: 361-367.
[12] Gho BC, Schoemaker RG, van den Doel MA, Duncker DJ and Verdouw PD. Myocardial protection by brief ischemia in noncardiac tissue. Circulation 1996; 94: 2193-2200.
[13] Wei M, Xin P, Li S, Tao J, Li Y, Li J, Liu M, Li J, Zhu W and Redington AN. Repeated remote ischemic postconditioning protects against adverse left ventricular remodeling and improves survival in a rat model of myocardial infarction. Circ Res 2011; 108: 1220-1225.
[14] Xin P, Zhu W, Li J, Ma S, Wang L, Liu M, Li J, Wei M and Redington AN. Combined local ischemic postconditioning and remote perconditioning recapitulate cardioprotective effects of local ischemic preconditioning. Am J Physiol Heart Circ Physiol 2010; 298: H1819-1831.
[15] Zhang JQ, Wang Q, Xue FS, Li RP, Cheng Y, Cui XL, Liao X and Meng FM. Ischemic preconditioning produces more powerful anti-inflammatory and cardioprotective effects than limb remote ischemic postconditioning in rats with myocardial ischemia-reperfusion injury. Chin Med J (Engl) 2013; 126: 3949-3955.
[16] Schmidt MR, Smerup M, Konstantinov IE, Shimizu M, Li J, Cheung M, White PA, Kristiansen SB, Sorensen K, Dzavik V, Redington AN and Kharbanda RK. Intermittent peripheral tissue ischemia during coronary ischemia reduces myocardial infarction through a KATP-dependent mechanism: first demonstration of remote ischemic perconditioning. Am J Physiol Heart Circ Physiol 2007; 292: H1883-1890.
[17] Gui D, Huang J, Liu W, Guo Y, Xiao W and Wang N. Astragaloside IV prevents acute kidney injury in two rodent models by inhibiting oxidative stress and apoptosis pathways. Apoptosis 2013; 18: 409-422.
[18] Zhang LY, Yi PF, Guo X, Wu SC, Fu YX, Zhang C, Fu BD, Shen HQ and Wei XB. Astragaloside IV Inhibits the Inflammatory Injury of Chicken Type II Pneumocytes Induced by Avian Pathogenic Escherichia coli. Inflammation 2016; 39: 1660-9.
[19] Wang S, Li J, Huang H, Gao W, Zhuang C, Li B, Zhou P and Kong D. Anti-hepatitis B virus activities of astragaloside IV isolated from radix Astragali. Biol Pharm Bull 2009; 32: 132-135.
[20] Tu L, Pan CS, Wei XH, Yan L, Liu YY, Fan JY, Mu HN, Li Q, Li L, Zhang Y, He K, Mao XW, Sun K, Wang CS, Yin CC and Han JY. Astragaloside IV protects heart from ischemia and reperfusion injury via energy regulation mechanisms. Microcirculation 2013; 20: 736-747.
[21] Zhao Y, Li Q, Zhao W, Li J, Sun Y, Liu K, Liu B and Zhang N. Astragaloside IV and cycloastragenol are equally effective in inhibition of endoplasmic reticulum stress-associated TXNIP/NLRP3 inflammasome activation in the endothelium. J Ethnopharmacol 2015; 169: 210-218.
[22] Qiu X, Guo Q, Xiong W, Yang X and Tang YQ. Therapeutic effect of astragaloside-IV on bradycardia is involved in up-regulating klotho expression. Life Sci 2016; 144: 94-102.
[23] Wang SG, Xu Y, Chen JD, Yang CH and Chen XH. Astragaloside IV stimulates angiogenesis and increases nitric oxide accumulation via JAK2/STAT3 and ERK1/2 pathway. Molecules 2013; 18: 12809-12819.
[24] Wang SG, Xu Y, Xie H, Wang W and Chen XH. Astragaloside IV prevents lipopolysaccharide-induced injury in H9C2 cardiomyocytes. Chin J Nat Med 2015; 13: 127-132.
[25] Alburquerque-Bejar JJ, Barba I, Inserte J, Miro-Casas E, Ruiz-Meana M, Poncelas M, Vilardosa U, Valls-Lacalle L, Rodriguez-Sinovas A and Garcia-Dorado D. Combination therapy with remote ischaemic conditioning and insulin or exenatide enhances infarct size limitation in pigs. Cardiovasc Res 2015; 107: 246-254.
[26] Fan Y, Yang S, Cao Y and Huang Y. Effects of acute and chronic atorvastatin on cardioprotection of ischemic postconditioning in isolated rat hearts. Cardiovasc Ther 2013; 31: 187-192.
[27] Gonon AT, Jung C, Yang J, Sjoquist PO and Pernow J. The combination of L-arginine and ischaemic post-conditioning at the onset of reperfusion limits myocardial injury in the pig. Acta Physiol (Oxf) 2011; 201: 219-226.
[28] Yamaguchi T, Izumi Y, Nakamura Y, Yamazaki T, Shiota M, Sano S, Tanaka M, Osada-Oka M, Shimada K, Miura K, Yoshiyama M and Iwao H. Repeated remote ischemic conditioning attenuates left ventricular remodeling via exosome-mediated intercellular communication on chronic heart failure after myocardial infarction. Int J Cardiol 2015; 178: 239-246.
[29] Aimo A, Borrelli C, Giannoni A, Pastormerlo LE, Barison A, Mirizzi G, Emdin M and Passino C. Cardioprotection by remote ischemic conditioning: Mechanisms and clinical evidences. World J Cardiol 2015; 7: 621-632.
[30] Shinde AV and Frangogiannis NG. Fibroblasts in myocardial infarction: a role in inflammation and repair. J Mol Cell Cardiol 2014; 70: 74-82.

[31] van den Borne SW, Diez J, Blankesteijn WM, Verjans J, Hofstra L and Narula J. Myocardial remodeling after infarction: the role of myofibroblasts. Nat Rev Cardiol 2010; 7: 30-37.
[32] Weber KT, Sun Y, Bhattacharya SK, Ahokas RA and Gerling IC. Myofibroblast-mediated mechanisms of pathological remodelling of the heart. Nat Rev Cardiol 2013; 10: 15-26.
[33] Che X, Wang Q, Xie Y, Xu W, Shao X, Mou S and Ni Z. Astragaloside IV suppresses transforming growth factor-beta1 induced fibrosis of cultured mouse renal fibroblasts via inhibition of the MAPK and NF-kappaB signaling pathways. Biochem Biophys Res Commun 2015; 464: 1260-1266.
[34] Qi Q, Mao Y, Yi J, Li D, Zhu K and Cha X. Anti-fibrotic effects of Astragaloside IV in systemic sclerosis. Cell Physiol Biochem 2014; 34: 2105-2116.
[35] Chen P, Xie Y, Shen E, Li GG, Yu Y, Zhang CB, Yang Y, Zou Y, Ge J, Chen R and Chen H. Astragaloside IV attenuates myocardial fibrosis by inhibiting TGF-beta1 signaling in coxsackievirus B3-induced cardiomyopathy. Eur J Pharmacol 2011; 658: 168-174.
[36] Li Y, Takemura G, Okada H, Miyata S, Maruyama R, Li L, Higuchi M, Minatoguchi S, Fujiwara T and Fujiwara H. Reduction of inflammatory cytokine expression and oxidative damage by erythropoietin in chronic heart failure. Cardiovasc Res 2006; 71: 684-694.
[37] Yang Y, Lv J, Jiang S, Ma Z, Wang D, Hu W, Deng C, Fan C, Di S, Sun Y and Yi W. The emerging role of Toll-like receptor 4 in myocardial inflammation. Cell Death Dis 2016; 7: e2234.
[38] Liu L, Wang Y, Cao ZY, Wang MM, Liu XM, Gao T, Hu QK, Yuan WJ and Lin L. Up-regulated TLR4 in cardiomyocytes exacerbates heart failure after long-term myocardial infarction. J Cell Mol Med 2015; 19: 2728-2740.
[39] Francis Stuart SD, De Jesus NM, Lindsey ML and Ripplinger CM. The crossroads of inflammation, fibrosis, and arrhythmia following myocardial infarction. J Mol Cell Cardiol 2016; 91: 114-122.
[40] Ripplinger CM, Lou Q, Li W, Hadley J and Efimov IR. Panoramic imaging reveals basic mechanisms of induction and termination of ventricular tachycardia in rabbit heart with chronic infarction: implications for low-voltage cardioversion. Heart Rhythm 2009; 6: 87-97.
[41] Timmers L, Sluijter JP, van Keulen JK, Hoefer IE, Nederhoff MG, Goumans MJ, Doevendans PA, van Echteld CJ, Joles JA, Quax PH, Piek JJ, Pasterkamp G and de Kleijn DP. Toll-like receptor 4 mediates maladaptive left ventricular remodeling and impairs cardiac function after myocardial infarction. Circ Res 2008; 102: 257-264.
[42] Timmers L, Pasterkamp G, de Hoog VC, Arslan F, Appelman Y and de Kleijn DP. The innate immune response in reperfused myocardium. Cardiovasc Res 2012; 94: 276-283.
[43] Abbate A, Bussani R, Amin MS, Vetrovec GW and Baldi A. Acute myocardial infarction and heart failure: role of apoptosis. Int J Biochem Cell Biol 2006; 38: 1834-1840.
[44] Kung G, Konstantinidis K and Kitsis RN. Programmed necrosis, not apoptosis, in the heart. Circ Res 2011; 108: 1017-1036.
[45] Tsujimoto Y and Shimizu S. Another way to die: autophagic programmed cell death. Cell Death Differ 2005; 12 Suppl 2: 1528-1534.
[46] Czabotar PE, Lessene G, Strasser A and Adams JM. Control of apoptosis by the BCL-2 protein family: implications for physiology and therapy. Nat Rev Mol Cell Biol 2014; 15: 49-63.
[47] Ardehali H, Sabbah HN, Burke MA, Sarma S, Liu PP, Cleland JG, Maggioni A, Fonarow GC, Abel ED, Campia U and Gheorghiade M. Targeting myocardial substrate metabolism in heart failure: potential for new therapies. Eur J Heart Fail 2012; 14: 120-129.
[48] Loukogeorgakis SP, Williams R, Panagiotidou AT, Kolvekar SK, Donald A, Cole TJ, Yellon DM, Deanfield JE and MacAllister RJ. Transient limb ischemia induces remote preconditioning and remote postconditioning in humans by a K(ATP)-channel dependent mechanism. Circulation 2007; 116: 1386-1395.